

pubs.acs.org/macroletters Letter

High-Resolution Nanopatterning of Free-Standing, Self-Supported Helical Polypeptide Rod Brushes via Electron Beam Lithography

Yuming Huang,§ Hai Tran,§ and Christopher K. Ober*



Cite This: ACS Macro Lett. 2021, 10, 755–759



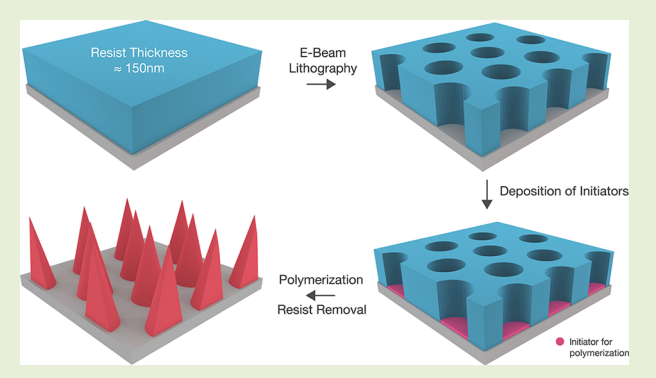
ACCESS

Metrics & More



Supporting Information

ABSTRACT: In this study of nanopatterned helical poly(benzyl-L-glutamate) (PBLG) brushes, rod-type brush arrays were fabricated via an integrated process of high-resolution lithography and surface-initiated vapor deposition polymerization (SI-VDP). "Nanospikes" of polymer brushes with spacings of less than 100 nm were produced. The topology and areal behavior of the resulting patterned rod-like brushes were analyzed and compared with patterned coil-type brushes. A geometric study of these self-assembled "nanospikes" was carried out, and their cross sections were investigated via focused ion beam (FIB) and scanning electron microscopy (SEM). Furthermore, the presence of poly(N-isopropylacrylamide) (PNIPAM) brushes in unpatterned regions was shown to inhibit undesired "inter-spike" bridging of the PBLG brushes, resulting in more well-defined



nanostructures. It was shown that rod-like polypeptide brushes are capable of self-segregation and become arranged vertically without any external support from their surroundings, to form a rod bundle end-point functional topography that could provide possible pathways for studies of model biological surfaces, directed assembly of nanoparticles, or binary mixed brush surfaces with dual properties.

Polymer brushes are typically polymer chains with one end anchored via stable covalent bonds to a substrate, such as silica. While polymer brushes have been an active research area for some years, precise control of the area-selective formation of these brushes remains a challenge, especially when nanoscale resolution is required. As such, there is growing interest in integrating lithographic techniques with polymer brush synthesis. Applications such as directed cell growth, substrates for cell-membrane derived sheets, thermoresponsive surfaces, and antibody biosensors have been developed in the past using patterned brushes with submicron structures.

In general, there are two approaches in generating patterned polymer brushes: the "top-down" approach, where the polymer brushes are grown homogeneously on the surface and then selectively removed to form a pattern; and the "bottom-up" approach, where a patterned self-assembled initiator monolayer is formed as the site for subsequent surface-initiated polymerization. While the "top-down" approach is more straightforward and uncomplicated in terms of chemical processing, it has several disadvantages, such as postprocessing residue, surface defects, and overetching. On the other hand, "bottom-up" approaches are usually associated with complications in terms of chemical compatibility and processing, since it involves a layer of patterned resist that forms the template that limits self-assembled monolayer (SAM) formation to a specific region. Thus, there are merits in developing a polymer brush

synthesis technique that is compatible with nanofabrication methods, especially high-resolution lithography process methods. In this study, we developed a facile "bottom-up" method for forming well-defined, self-supported rod polymer brushes patterned on the nanoscale using a sequence of electron beam lithography (EBL) and vapor phase surface-initiated polymerization.

Due to their thermodynamically stable conformation and high persistence length, α -helical polypeptide brushes were used as model rod brushes. ¹⁶ Polypeptides are also known to offer potential benefits in biological applications, ^{17,18} and the vertical alignment of these brushes combined with their unidirectional vapor growth can enable terminal group functionalization and, thus, specific surface chemical properties. Our previous research has already shown the vertical alignment and self-aggregation of polypeptide brushes when placed in a mixed rod—coil brushes system. However, the poly- γ -benzyl-L-glutamate (PBLG) brushes' self-support and freestanding capability were not examined in the same study due

Received: March 21, 2021 **Accepted:** May 6, 2021 **Published:** May 31, 2021





Scheme 1. Synthesis of (a) PBLG Brushes via SI-ROP, (b) PS via SI-CuCRP, and (c) PNIPAM via SI-ATRP

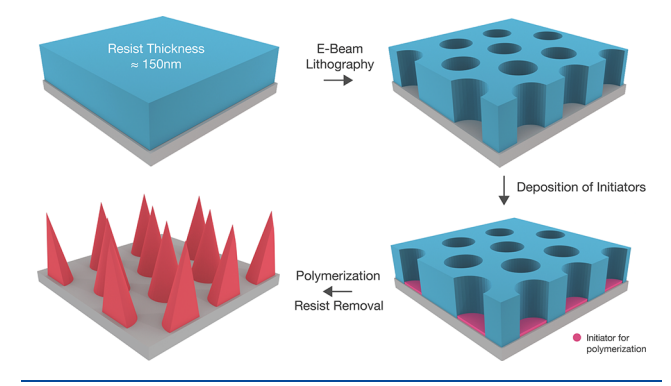
to a lack of nanopatterning analysis.¹⁹ It is worth noting that the fundamental characteristics of nanopatterned polymer brushes (NPB) are different from those of homogeneous brush layers and micropatterned brushes since the NPB's polymer contour length now becomes comparable to pattern size.^{20–22} Therefore, it was of interest to investigate helical polypeptide NPBs and gain insight into how nanostructured rod-type polymer brushes adapt to the imposition of nanoscale patterns.

Moreover, the polypeptide brushes' self-supported, controlled surface topography with uniform end-group functionality and submicron spacing superficially resembles the capsid and antigen structure of several types of viruses, which are responsible for cell recognition and invasion and antibody recognition.²³ As such, it would be possible for us to make a virus-like surface using proteins for cell-virus interaction simulations if the spacings could be made small enough. It was therefore of interest to us to understand how much control we have over the architecture and constituents of such polymer brushes and what periodic spacings we can achieve in producing this model surface system. With the ability to control the placement, spacing, and molecular arrangement of these polypeptide brushes at the nanometer scale via EBL, in the future we want to use them to study biomolecular surface attachment and cell-surface interactions that involve feature sizes in the sub-50 nm regime.

In order to test the control of our processes as well as to examine the self-aggregation behavior of polypeptides under different conditions, polymer brushes with various thicknesses, patterns, and structures were grown for a comparative study. Specifically, PBLG brushes were synthesized via surfaceinitiated ring-opening polymerization (SI-ROP) and poly(Nisopropylacrylamide) (PNIPAM) were separately grown via surface-initiated atom transfer radical polymerization (SI-ATRP) as secondary brushes in a binary brush synthesis (Scheme 1). As noted above, electron beam lithography was used to create patterned amino silane initiators, where a JEOL 9500 EBL system was used to expose a ZEP-520A e-beam resist film (~150 nm) on a blank silicon wafer. The patterned resist film was used to mask initiator deposition after a brief descum process via reactive ion etching. Afterward, vapor deposition of (3-aminopropyl)di-isopropylethoxysilane (AP-DIPES) was carried out following the procedure suggested by Fetterly et al.²⁴ The substrate and APDIPES were placed together in a closed chamber with a pressure of 1 Torr and a temperature of 70 $^{\circ}$ C. APDIPES was selected due to its bulky size to localize surface deposition to the exposed oxide surface

and to minimize transport of APDIPES through the resist film. Vapor-deposition conditions were further optimized to prevent background contamination of the silane in unexposed areas. After the resist lift-off, PBLG brushes were grown via vapor phase SI-ROP under vacuum and elevated temperature, and the solvent quenching process was used via the procedure described by Tran et al. (Chart 1).

Chart 1. Formation of Nanopatterned Brushes via EBL



Topological studies of these polymer brushes were done by the Zeiss Ultra scanning electron microscope (SEM) and Asylum MFP-3D atomic force microscopy (AFM). Figure 1a—d shows the brushes fabricated with dot-like EBL patterns: the center-to-center distance was held at 200 nm, and the diameters of the dot-patterned brushes are around 60 nm (Figure 1a,b for PBLG and Figure 1c for PS) and 100 nm (Figure 1d for PBLG). As the diameter of the dots increases, the PBLG brushes form separate bundles, reflecting the inhomogeneous segregation of these brushes. Furthermore, the brushes start to interact with each other and form "bridges" between each other at larger spikes, probably due to a decrease in edge-to-edge distance (Figure 1d). However, "bridges" only formed between edge-adjacent dots, but not if the regions were located on the diagonals.

A simple explanation is that a diagonal is always ~1.41× more distant than an edge, which makes the "inter-spike" interaction more difficult. One noteworthy observation is that the polypeptide brushes can stand up on their own without any secondary support, probably due to their high persistence length (~70 nm)²⁵ and strong intermolecular interactions. A comparison between PBLG brushes and PS brushes further demonstrates this characteristic of the rod brushes. For

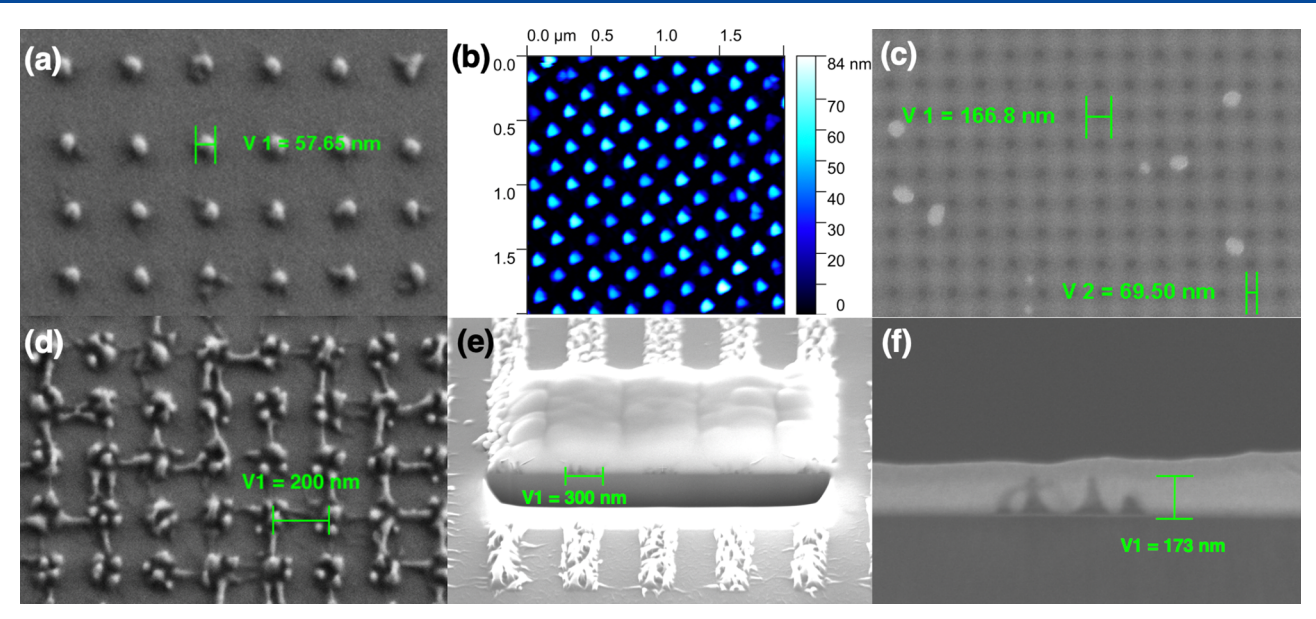


Figure 1. SEM image of PBLG brushes with diameter (a) \sim 60 nm and (b) the corresponding AFM images. (c) SEM image of PS brushes with diameters of \sim 70 nm for the inner circle and \sim 160 nm for the outer circle. (d) SEM image of PBLG brushes with diameters of \sim 100 nm showing the inhomogeneous aggregation. (e) SEM images of FIB processing for cross-sectional analysis and (f) SEM image of PBLG brushes cross-sectional. V1 and V2 are dummy labels for length measurements.

comparison, patterned PS brushes were fabricated through similar procedures described in Chart 1, with one additional step for attaching 2-bromo-2-methylpropionyl bromide (BiBB) onto the aminosilane initiator (Scheme 1b). Figure 1c illustrates the SEM image of patterned PS brushes fabricated via surface-initiated Cu(0) mediated controlled radical polymerization (SI-CuCRP) with the same resist template as the PBLG brushes in Figure 1a: the edge of the resulting PS brushes became blurry and diffuse, which is in agreement with previous studies, ^{21,26} and is consistent with the collapse of the brushes at the edges of the patterns due to low polymer persistence length combined with the absence of strong interchain interactions.

While SEM images provide insights on the topology of the brushes, they have been limited in assessing more geometric information such as the height and the cross-sectional shapes of the PBLG brushes. Figure 1b shows the corresponding AFM image of the brushes in Figure 1a using an Asylum MFP-3D. The average brush height is 60 nm, and cone-shaped tips were observed. In order to obtain a more comprehensive understanding of the shape of these "nanospikes", a cross-sectional study was carried out using the Helios G4 UX Focused Ion Beam (FIB) to isolate samples for side view observation. PBLG brushes with line pattern was prepared and protected by depositing a layer of platinum on top. Subsequently, the sample was cut by a strong focused ion beam in the direction normal to the plane of the substrate until a very thin slice was obtained. The entire process was monitored via SEM imaging (Chart S1). Figure 1e,f shows a cross-section of the PBLG brushes after processing. Instead of straight sides shown in AFM images, the side of the spikes curved inward, which reflect a nonlinear relationship between the collapse tendency of the brushes and height.

While patterned PBLG brushes exhibit high orientation and specific surface functionality with potential for biological applications, the addition of secondary brushes can further modify the surface with unique dual properties. ^{27–29} For this purpose, SI-ATRP was integrated after the fabrication of

patterned PBLG brushes to grow the secondary brushes at the blank area on the same substrate. PNIPAM was selected for the secondary brush in this case due to its compatibility with SI-ATRP³⁰ as well as its stimulus responsive properties: as PNIPAM established a change in solubility in water at its lower critical solution temperature (LCST) of 32 °C, 31 one can control the swelling of the PNIPAM film in solution to expose or envelop the spiky rod brushes by controlling the surrounding temperature. However, for the purpose of this study, we focus on how the presence of secondary brushes can isolate and potentially support the PBLG "nanospikes". The secondary brush synthesis was carried out via a two-step procedure. ATRP initiators were immobilized into nonpatterned areas by immersing the sample into a solution of BiBB-functionalized silanes overnight at room temperature; SI-ATRP was then carried out for PNIPAM brush growth in the desired area (Scheme 1c). The resulting binary brush sample was then analyzed by SEM and AFM and compared with the PBLG homobrush sample in Figure 2. The height of PNIPAM brushes was measured as 25 nm using ellipsometry. Instead of a spiky surface with clean, sharp nanocones, the surface after PNIPAM brushes growth is smoother; the secondary brushes filled the blank area, causing the edges to be less defined. Also, the addition of PNIPAM brushes improved phase separation, which is reflected by the decrease in the number of "bridges" between the nanocones and bundles within each area. Additionally, the same sample was scratched to remove brush from the region of the scratch and examined using SEM imaging to provide a more visual comparison of the relative height of the PNIPAM, and PBLG brushes on the silicon surface (Figure S1) to confirm the ellipsometer readings of the presence of secondary PNIPAM brushes in the open area, which might not be directly noted in Figure 2.

Herein, we report the preparation of patterned polypeptide brushes via SI-ROP following EBL patterned initiator formation. This work combined distinct techniques from the areas of oxide surface functionalization using organosilane monolayers with e-beam nanolithography to achieve nanoscale

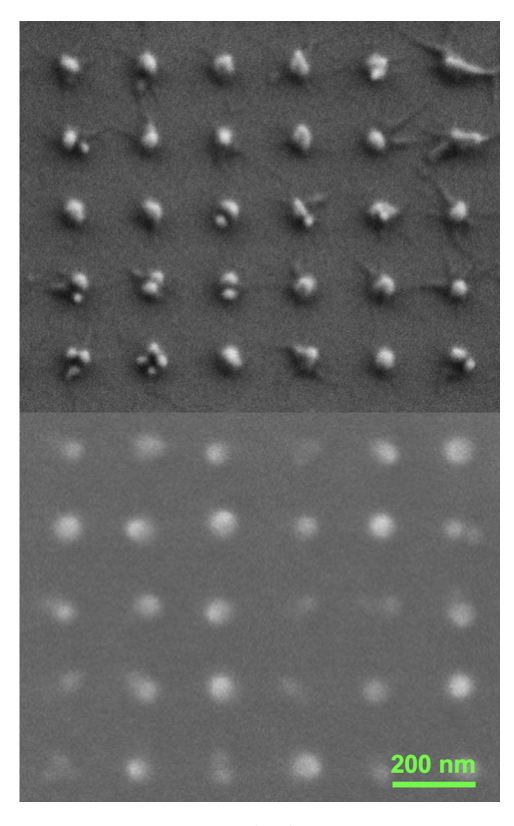


Figure 2. PBLG homobrushes (top) and PBLG/PNIPAM mixed brushes (bottom). The magnification is the same for both images.

localized functionalization, combining surface-initiated polymer brush growth to form polymer thin films. Patterned PBLG brushes with diameters of 60–100 nm were produced, and vertically oriented "nanospikes" were formed after a solvent quenching process. In contrast, PS brushes showed a collapsed morphology due to the coil polymer's lower persistence length (~1 nm). In addition, PNIPAM brushes were grown in the "blank" areas to make patterned binary rod—coil brushes for stimuli-responsive surfaces.

It is a future goal to study how surface-modification of the end functional patterned rod brushes can form precisely placed, controlled attachments and the performance of such functional films. For example, with such materials it is possible to foresee the formation of functional arrays on desired surfaces with the assistance of the patterned brushes, where the active functional groups on the tips of the brushes act as specific binding sites of nanoparticles.³³ Such arrays could be the building blocks of the functional optical, electrical, sensor, or chemical devices^{34,35} or high-density magnetic storage medium.^{36,37}

The mild conditions of vapor phase deposition make this method particularly useful in combination with the EBL for the patterning procedure. The bottom-up patterning method reduces process defects and allows polymer films to remain intact compared to top-down approaches where films are etched after being made. Furthermore, the grafting-from synthesis approach, that is, surface-initiated polymerization, results in high grafting density and controlled and uniform film thickness, thus, achieving enhanced self-assembly of the mixed rod—coil polymer brushes. Combining with a solvent quenching process¹⁹ significantly reduced the annealing time compared to the thermal or solvent annealing techniques

compared to block copolymer self-assembly. Further studies are required for understanding the mechanism of such attachments and finer control on these assemblies to produce patterned rod-brush structures with smaller spacings and explore their possible applications in biological simulations and electronic devices.

ASSOCIATED CONTENT

Supporting Information

The Supporting Information is available free of charge at https://pubs.acs.org/doi/10.1021/acsmacrolett.1c00187.

Materials and Methods; SEM image of the scratched area for binary brushes surface analysis; FIB processing for cross sectional analysis (PDF)

AUTHOR INFORMATION

Corresponding Author

Christopher K. Ober — Department of Materials Science and Engineering, Cornell University, Ithaca, New York 14853, United States; orcid.org/0000-0002-3805-3314; Email: cko3@cornell.edu

Authors

Yuming Huang — Department of Materials Science and Engineering, Cornell University, Ithaca, New York 14853, United States; orcid.org/0000-0002-1617-8570

Hai Tran — Robert F. Smith School of Chemical and Biomolecular Engineering, Cornell University, Ithaca, New York 14853, United States

Complete contact information is available at: https://pubs.acs.org/10.1021/acsmacrolett.1c00187

Author Contributions

⁸These authors contributed equally to this work. The manuscript was written through contributions of all authors. C.K.O., Y.H.., and H.T. planned the research; H.T. performed surface-initiated reactions and AFM measurements with the assistance of Y.H.; Y.H. performed cleanroom-related nanofabrication and SEM characterizations including FIB processing. All authors have given approval to the final version of the manuscript.

Funding

This work is supported by the National Science Foundation (DMR-1905403).

Notes

The authors declare no competing financial interest.

ACKNOWLEDGMENTS

We would like to acknowledge the excellent support on EBL conditions and SEM imaging from Cornell CNF staff members, Alan Bleier and Amrita Banerjee. We would also like to acknowledge the assistance from Malcolm Thomas with FIB processing in the CCMR facility. This work made use of a Helios FIB supported by NSF (DMR-1539918), the Cornell Center for Materials Research Shared Facilities, which are supported through the NSF MRSEC Program (DMR1719875), and the Cornell NanoScale Facility, a member of the National Nanotechnology Coordinated Infrastructure (NNCI), which is supported by the National Science Foundation (Grant NNCI-2025233).

REFERENCES

- (1) Barbey, R.; Lavanant, L.; Paripovic, D.; Schuwer, N.; Sugnaux, C.; Tugulu, S.; Klok, H. A. Polymer brushes via surface-initiated controlled radical polymerization: synthesis, characterization, properties, and applications. *Chem. Rev.* **2009**, *109* (11), 5437–527.
- (2) Zhou, Z.; Yu, P.; Geller, H. M.; Ober, C. K. Biomimetic polymer brushes containing tethered acetylcholine analogs for protein and hippocampal neuronal cell patterning. *Biomacromolecules* **2013**, *14* (2), 529–37.
- (3) Kollarigowda, R. H.; Fedele, C.; Rianna, C.; Calabuig, A.; Manikas, A. C.; Pagliarulo, V.; Ferraro, P.; Cavalli, S.; Netti, P. A. Light-responsive polymer brushes: active topographic cues for cell culture applications. *Polym. Chem.* **2017**, *8* (21), 3271–3278.
- (4) Chen, L.; Yan, C.; Zheng, Z. Functional polymer surfaces for controlling cell behaviors. *Mater. Today* **2018**, 21 (1), 38–59.
- (5) Liu, H. Y.; Chen, W. L.; Ober, C. K.; Daniel, S. Biologically Complex Planar Cell Plasma Membranes Supported on Polyelectrolyte Cushions Enhance Transmembrane Protein Mobility and Retain Native Orientation. *Langmuir* **2018**, *34* (3), 1061–1072.
- (6) Yu, Q.; Johnson, L. M.; López, G. P. Nanopatterned Polymer Brushes for Triggered Detachment of Anchorage-Dependent Cells. *Adv. Funct. Mater.* **2014**, 24 (24), 3751–3759.
- (7) Jones, D. M.; Smith, J. R.; Huck, W. T. S.; Alexander, C. Variable Adhesion of Micropatterned Thermoresponsive Polymer Brushes: AFM Investigations of Poly(*N*-isopropylacrylamide) Brushes Prepared by Surface-Initiated Polymerizations. *Adv. Mater.* **2002**, *14* (16), 1130.
- (8) Kaholek, M.; Lee, W.-K.; LaMattina, B.; Caster, K. C.; Zauscher, S. Fabrication of Stimulus-Responsive Nanopatterned Polymer Brushes by Scanning-Probe Lithography. *Nano Lett.* **2004**, *4* (2), 373–376.
- (9) de las Heras Alarcón, C.; Farhan, T.; Osborne, V. L.; Huck, W. T. S.; Alexander, C. Bioadhesion at micro-patterned stimuli-responsive polymer brushes. *J. Mater. Chem.* **2005**, *15* (21), 2089.
- (10) Welch, M. E.; Xu, Y.; Chen, H.; Smith, N.; Tague, M. E.; Abruna, H. D.; Baird, B.; Ober, C. K. Polymer Brushes as Functional, Patterned Surfaces for Nanobiotechnology. *J. Photopolym. Sci. Technol.* **2012**, 25 (1), 53–56.
- (11) Welch, M. E.; Ritzert, N. L.; Chen, H.; Smith, N. L.; Tague, M. E.; Xu, Y.; Baird, B. A.; Abruna, H. D.; Ober, C. K. Generalized platform for antibody detection using the antibody catalyzed water oxidation pathway. *J. Am. Chem. Soc.* **2014**, *136* (5), 1879–83.
- (12) Krishnamoorthy, M.; Hakobyan, S.; Ramstedt, M.; Gautrot, J. E. Surface-initiated polymer brushes in the biomedical field: applications in membrane science, biosensing, cell culture, regenerative medicine and antibacterial coatings. *Chem. Rev.* **2014**, *114* (21), 10976–1026.
- (13) Chen, W. L.; Cordero, R.; Tran, H.; Ober, C. K. 50th Anniversary Perspective: Polymer Brushes: Novel Surfaces for Future Materials. *Macromolecules* **2017**, *50* (11), 4089–4113.
- (14) Schuh, C.; Santer, S.; Prucker, O.; Rühe, J. Polymer Brushes with Nanometer-Scale Gradients. *Adv. Mater.* **2009**, 21 (46), 4706–4710.
- (15) Yu, Q.; Ista, L. K.; Gu, R.; Zauscher, S.; Lopez, G. P. Nanopatterned polymer brushes: conformation, fabrication and applications. *Nanoscale* **2016**, 8 (2), 680–700.
- (16) Shen, Y.; Li, Z.; Klok, H.-A. Polypeptide brushes grown via surface-initiated ring-opening polymerization of α -amino acid N-carboxyanhydrides. *Chin. J. Polym. Sci.* **2015**, 33 (7), 931–946.
- (17) Kar, M.; Pauline, M.; Sharma, K.; Kumaraswamy, G.; Sen Gupta, S. Synthesis of poly-L-glutamic acid grafted silica nanoparticles and their assembly into macroporous structures. *Langmuir* **2011**, *27* (19), 12124–33.
- (18) Ma, Y.; Shen, Y.; Li, Z. Different cell behaviors induced by stereochemistry on polypeptide brush grafted surfaces. *Materials Chemistry Frontiers* **2017**, *1* (5), 846–851.
- (19) Tran, H.; Zhang, Y.; Ober, C. K. Synthesis, Processing, and Characterization of Helical Polypeptide Rod-Coil Mixed Brushes. *ACS Macro Lett.* **2018**, *7* (10), 1186–1191.

- (20) Lee, W. K.; Patra, M.; Linse, P.; Zauscher, S. Scaling behavior of nanopatterned polymer brushes. *Small* **2007**, 3 (1), 63–6.
- (21) Ahn, S. J.; Kaholek, M.; Lee, W. K.; LaMattina, B.; LaBean, T. H.; Zauscher, S. Surface-initiated polymerization on nanopatterns fabricated by electron-beam lithography. *Adv. Mater.* **2004**, *16* (23–24), 2141–2145.
- (22) Chen, W. L.; Menzel, M.; Watanabe, T.; Prucker, O.; Ruhe, J.; Ober, C. K. Reduced Lateral Confinement and Its Effect on Stability in Patterned Strong Polyelectrolyte Brushes. *Langmuir* **2017**, 33 (13), 3296–3303.
- (23) Haywood, A. M. Virus receptors: binding, adhesion strengthening, and changes in viral structure. *J. Virol.* **1994**, *68* (1), 1–5.
- (24) Fetterly, C. R.; Olsen, B. C.; Luber, E. J.; Buriak, J. M. Vapor-Phase Nanopatterning of Aminosilanes with Electron Beam Lithography: Understanding and Minimizing Background Functionalization. *Langmuir* **2018**, 34 (16), 4780–4792.
- (25) Zhang, G.; Fournier, M. J.; Mason, T. L.; Tirrell, D. A. Toward Monodisperse Poly(γ -benzyl α ,L-glutamate): Uniform, Polar, Molecular Rods. *MRS Proc.* **1991**, *255*, na.
- (26) Rastogi, A.; Paik, M. Y.; Tanaka, M.; Ober, C. K. Direct patterning of intrinsically electron beam sensitive polymer brushes. *ACS Nano* **2010**, *4* (2), 771–80.
- (27) Zhou, F.; Zheng, Z.; Yu, B.; Liu, W.; Huck, W. T. Multicomponent polymer brushes. *J. Am. Chem. Soc.* **2006**, *128* (50), 16253–8.
- (28) Sweat, D. P.; Kim, M.; Yu, X.; Schmitt, S. K.; Han, E.; Choi, J. W.; Gopalan, P. A dual functional layer for block copolymer self-assembly and the growth of nanopatterned polymer brushes. *Langmuir* **2013**, 29 (41), 12858–65.
- (29) Pallandre, A.; Glinel, K.; Jonas, A. M.; Nysten, B. Binary Nanopatterned Surfaces Prepared from Silane Monolayers. *Nano Lett.* **2004**, *4* (2), 365–371.
- (30) Mandal, K.; Balland, M.; Bureau, L. Thermoresponsive micropatterned substrates for single cell studies. *PLoS One* **2012**, 7 (5), e37548.
- (31) Jain, K.; Vedarajan, R.; Watanabe, M.; Ishikiriyama, M.; Matsumi, N. Tunable LCST behavior of poly(N-isopropylacrylamide/ionic liquid) copolymers. *Polym. Chem.* **2015**, *6* (38), 6819–6825.
- (32) Brûlet, A.; Boué, F.; Cotton, J. P. About the Experimental Determination of the Persistence Length of Wormlike Chains of Polystyrene. *J. Phys. II* **1996**, *6* (6), 885–891.
- (33) Wu, D. Y.; Käfer, F.; Diaco, N.; Ober, C. K. Silica-PMMA hairy nanoparticles prepared via phase transfer-assisted aqueous miniemulsion atom transfer radical polymerization. *J. Polym. Sci.* **2020**, 58, 2310
- (34) Zhang, H.; Cadusch, J.; Kinnear, C.; James, T.; Roberts, A.; Mulvaney, P. Direct Assembly of Large Area Nanoparticle Arrays. *ACS Nano* **2018**, *12* (8), 7529–7537.
- (35) Shipway, A. N.; Katz, E.; Willner, I. Nanoparticle Arrays on Surfaces for Electronic, Optical, and Sensor Applications. *Chem-PhysChem* **2000**, *1* (1), 18–52.
- (36) Ross, C. A. Patterned Magnetic Recording Media. *Annu. Rev. Mater. Res.* **2001**, 31 (1), 203–235.
- (37) Wen, T.; Zhang, D.; Wen, Q.; Zhang, H.; Liao, Y.; Li, Q.; Yang, Q.; Bai, F.; Zhong, Z. Magnetic nanoparticle assembly arrays prepared by hierarchical self-assembly on a patterned surface. *Nanoscale* **2015**, 7 (11), 4906–11.